Effect of Axial Compression on Flexural Hinge Rotation Capacity

Influence de l'effort normal sur la capacité de rotation des rotules plastiques

Der Einfluss der Normalkraft auf die Rotationsfähigkeit von plastischen Biegegelenken

M. Saeed MIRZA
Associate Professor of Civil Engineering
and Applied Mechanics and Dean of Students

John O. McCUTCHEON
Professor of Civil Engineering
and Applied Mechanics

McGill University
Montreal, Canada

INTRODUCTION

All limit design methods are based on the assumption that some sections of a statically indeterminate structure can attain a certain limiting moment value (M_u) dependent on the structure and loading geometry, cross-section details, reinforcement ratio, concrete strength, etc. When this maximum value of bending moment is approached, curvatures at this section and in its immediate vicinity increase very significantly and lead to the formation of the so-called "flexural hinge". It has been established by several investigators that complete redistribution of bending moments in a statically indeterminate structure occurs only if the hinging sections are capable of undergoing sufficient rotation. The rotation capacity of a flexural hinge decreases with an increase in the tension reinforcement and it has been shown to increase significantly if the concrete at the flexural fringe is confined by closely spaced lateral ties. Presence of axial compressive or tensile forces is known to modify the behaviour of a flexural hinge. However very little research work has been undertaken in this area of limit design.

This paper presents the results of an analytical experimental investigation (1) on twenty specimens with symmetrically reinforced square sections to examine the influence of longitudinal steel percentage and axial compression on rotation capacity of the so-called flexural hinges in beams and columns in statically indeterminate systems. These beams and eccentrically loaded

columns had a constant cross-section of 4 in. by 4 in. and a constant moment zone was maintained over a minimum length of 10 ins. in both types of specimens (Fig.1). Two reinforcing steel percentages (p = p' = 1.37 per cent for Series S1 and p = p' = 2.06 per cent for Series S2) were used in this investigation and two identical specimens were tested for each loading combination to verify the reproduc bility of results. The eccentric column loading brackets and the beam ends were heavily reinforced to eliminate any possibility of shear failures in these regions. The concrete strength and the lateral reinforcement were kept constant in all specimens which were tested under varying eccentricities giving a wide range of loadings from pure axial compressive loads to the case of pure bending.

ANALYTICAL METHOD

Once the curvature distribution along a member is established the rotation between any two sections can be evaluated by simple integration. The relationship between the bending moment and the curvature at a section is principally a function of the cross-section characteristics. Variation of the flexural rigidity along the span on account of cracking complicates the curvature calculations in cracked reinforced concrete members. For a member subjected to a constant bending moment the curvature varies from a maximum value at the cracked section to a mimimum at a point between the cracks.

Existing research data on cracking of concrete lead the assumption that the average spacing of cracks ΔL_{av} is 1.8 times the minimum spacing ΔL_{min} and the following expression was derived in Reference 1:

$$\Delta L_{av} = \frac{\phi}{\gamma} (1 + 0.1 \frac{B_f}{A_s})$$ (1)

where ϕ = the bar diameter

γ = a coefficient. For plain bars γ= 1 and for deformed bars = 1.6

A_s = cross-sectional area of tension reinforcement

and B_f = twice the area of the concrete cover.

Average crack spacing, evaluated using equation (1), was noted to be 2.5 in. for Series S1 and 2.0 in. for Series S2, which agreed well with the experimental results (Ref.1).

The following assumptions were made in evaluating the moment-curvature relationships:
1. At any load level, the compressive strain at the extreme fibre is assumed to be uniform along the reference length of 10 inches at a maximum concrete strain value. Strain distribution across a section was assumed to be linear.

2(a) The maximum compressive stress fc" was assumed to be (Ref.2)

$$f_c" = 0.85 \ f_c'$$ (2)

where f_c' = 28-day concrete compressive strength obtained from tests on 6 x 12 in. cylinders.

(b) As recommended by Hognestad (2), the maximum concrete compressive strain was assumed to be 0.0038.

3. The minimum curvature at a section between two cracks

$$\varepsilon_u / (^d/_2)$$

4. The maximum curvature over a crack can be determined using the method to be described later.

5. Knowing the maximum and minimum curvatures, the curvature distribution along the reference length can be established for rotating evaluation.

The concrete stress-strain curve shown in Fig.2 is given by the following equations:

(i) For $\varepsilon < \varepsilon_o$ = 0.002

$$f_c = f_c"[2^\varepsilon/\varepsilon_o - (^\varepsilon/\varepsilon_o)^2]$$ (3)

(ii) For $0.002 < \varepsilon < 0.0038$

$$f_c = f_c" - \frac{250}{3} fc"(\varepsilon - 0.002)$$ (4)

The compressive force C at any stress level f_c (Fig.) is given by

$$C = K_1 \varepsilon f_c"$$ (5)

with the resultant located at a distance $K_2\varepsilon$ from the extreme compression fibre.

For $\varepsilon < 0.002$, $K_1 = \frac{\varepsilon}{\varepsilon_o}(1 - \frac{\varepsilon}{3\varepsilon_o})$ (6)

and $K_2 = \dfrac{4 - ^\varepsilon/\varepsilon_o}{12(1 - \frac{\varepsilon}{3\varepsilon_o})}$ (7)

For $\varepsilon = \varepsilon_u$ = 0.0038, Obeid (1) derived the following values for K_1 and K_2:

$$K_1 = 0.79 \qquad \text{and} \qquad K_2 = 0.40$$ (8)

The ultimate compressive force C_u is given by

$$C_u = K_1 b \ f_c" \ n_u$$ (9)

where n_u = depth of the neutral axis at ultimate load.

The ultimate curvature ϕ_u is given by

$$\phi_u = \frac{\varepsilon_u}{n_u} \qquad (10)$$

Substituting from equation (10) into equation (9), the ultimate axial compressive load P_u is given by

$$\qquad (11)$$

$$P_u = C_u = K_1 bfc'' \varepsilon_u \left(\frac{1}{\phi_u} \right)$$

Substituting values of K_1, b, ε_u and f_c'', equation (11) becomes

$$P_u = \frac{1}{20} \left(\frac{1}{\phi_u} \right) \text{ kips} \qquad (12)$$

and $\quad M_u = P_u e = \frac{1}{20} \left(\frac{e}{\phi_u} \right) \text{ kip-in.} \qquad (13)$

Similar equations have been derived in Reference 1 for the conditions at yielding of tension reinforcement and for the case of pure flexure. Curvature and rotation values for the different specimens at yielding of tension steel and at ultimate load, calculated using the above method are detailed and compared with experimental results in Table 1 and are presented graphically in Figures 3 through 5.

EXPERIMENTAL PROCEDURE

Strain gauges were installed at the top and at the side of the concrete compressive zone and on the steel bars. Strains and deflections were recorded continuously using an automatic recorder. Curvature was calculated from the strain values using the equation

$$\phi = \frac{\varepsilon_c + \varepsilon_s}{d}$$

where ε_c is the compressive strain on the extreme concrete fibre and ε_s is the tensile strain in steel reinforcement. Rotation over a reference length of 10 inches was measured using rotation arms and two DCDT's (direct current differential transducers). Rotation values were also calculated by an integration of the experimental curvature values over the reference length.

All specimens were tested either in a 400,000 lb. capacity Baldwin - Lima - Hamilton universal testing machine or in a 60,000 lb. capacity Riehle universal testing machine. The load was applied in suitable increments at preselected eccentricity values (Table 1) through a ball and socket arrangement.

The following three distinct failure modes were observed in this investigation:
(i) Compression failures: (e.g. Specimen S1-1):Failure occurred during the crushing and spalling of the concrete cover on the compression side after compression steel had yielded. Tension steel did not show any signs of yielding. Signs of distress

in concrete were initially observed at loads ranging between 80 and 95 per cent of the ultimate load. Spalling of concrete was immediately followed by buckling of the compression steel.

(ii) **Balanced failure mode (Specimen S2-3):**

This mode of failure consisted generally of the yielding of the compression reinforcement, accompanied almost immediately by the yielding of the tension reinforcement and followed by a crushing of concrete in compression zone as the applied deformations were increased without any further increase of load.

(iii) **Flexural mode of failure (Specimen S1-4):**

General behaviour of these specimens was typical of under-reinforced beams due to yielding of the tension reinforcement. These specimens showed significantly larger deformations and ductility than those in cases (ii) and (i) above. Beam specimens tested under pure flexure (axial force P=0) showed the largest ductility which was observed to increase as the applied compressive loads were decreased from the pure axial compression capacity (at zero eccentricity) to zero for the case of pure flexure.

Comparison of Computed and Experimental Data:

The computed axial load and bending moments at ultimate load are compared with the experimental values in Table 1. A generally good agreement can be noted. Comparison of calculated curvature values at yield show good agreement with the experimental data. The curvature values at ultimate load were obtained from the last reading from the strain gauges before they become inoperational and therefore the calculated values are generally larger than the experimental ones. It may be noted that near ultimate load, strain values of the order of 0.006 were recorded which makes conservative the maximum strain value of 0.003 specified by the various codes.

Rotation and deflections were recorded continuously up to the ultimate load using DCDT's. Good correlation can be noted in the calculated and experimental values detailed in Table 1.

An examination of test data on all 20 test specimens shows that the available rotation capacity was not dependent on the steel percentages used. The rotation capacity was a maximum for the case of pure flexure and it decreased gradually by approximately 25 per cent as the applied axial compression load was increased to a point where a balanced failure condition was obtained. Further increase in the applied compression loads decreased the available rotation capacity at the hinge more rapidly to zero for the case of pure axial compression (eccentricity = 0). This trend was also noted in the computed results which show satisfactory agreement with the experimental data.

CONCLUSIONS

The results of this investigation can be summarized as follows:

1. Suitable equations have been developed to accurately predict axial force – bending   moment – curvature characteristics. Good agreement was obtained between the calculated strength and deformation values and the corresponding experimental data.

2. Maximum compressive strains of the order of 0.006 existed at extreme fibres near ultimate load, suggesting that larger deformations can be sustained at the so-called "flexural hinges". This would lead to a higher degree of moment redistribution in statically indeterminate reinforced concrete systems, which constitutes the basis of limit design.

3. Rotation capacity of the "flexural hinge" was not significantly influenced by the longitudinal steel percentage and was a maximum for the case of pure flexure.

4. Analytical and experimental results show that the available rotation capacity decreased by approximately 25 per cent as the axial compressive load was increased from zero to a point where balanced column failure resulted. Beyond the balance point, available hinge rotation diminished gradually becoming zero for the case of pure axial compression.

REFERENCES

1. E. Obeid, "Compression Hinges in Reinforced Concrete Elements", M.Eng. Thesis, McGill University, September 1969.

2. E. Hognestad, "A Study of Combined Bending and Axial Load in Reinforced Concrete Members", Research Bulletin Series No. 399, University of Illinois, November 1951.

Fig. 4. Comparison of Calculated and Measured Ultimate Curvature versus Ultimate Axial Load.
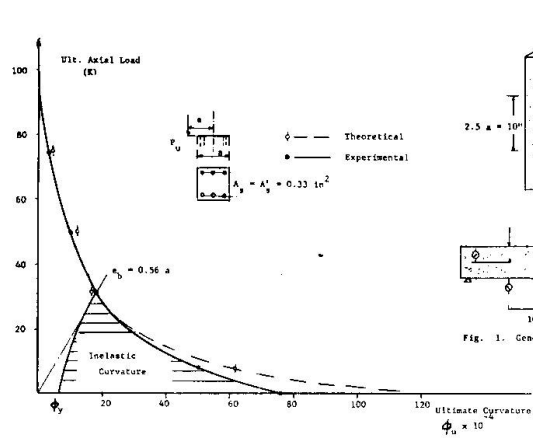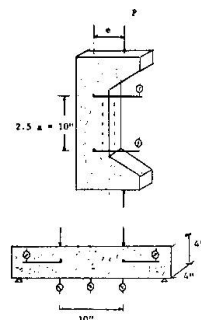

Fig. 1. General Arrangement.

Fig. 2. Assumed Stress-Strain Diagram of Concrete in Combined Axial Load and Bending.
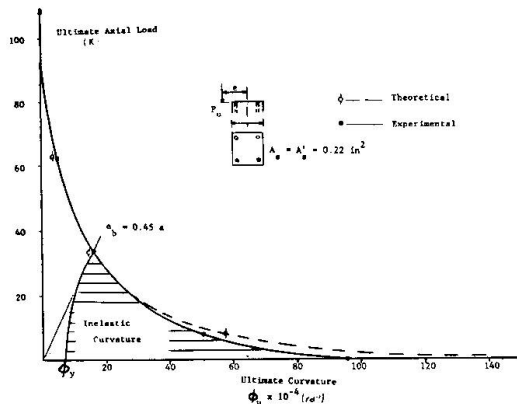

Fig. 3. Comparison of Calculated and Measured Ultimate Curvature versus Ultimate Axial Load.
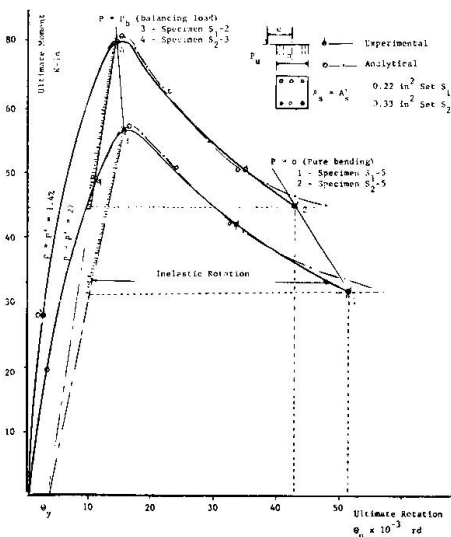

Fig. 5. Comparison of Calculated and Measured Ultimate Rotation, Axial Load and Moment.

Ult. Axial Load
(K)

ϕ —— Theoretical

$\bullet$ —— Experimental

$A_s = A_s' = 0.33$ in^2

$a_b = 0.56$ a

Inelastic Curvature

Ultimate Curvature
$\phi_u \times 10$

Fig. 4. Comparison of Calculated and Measured Ultimate Curvature versus Ultimate Axial Load.

Ultimate Axial Load
(K)

ϕ —— Theoretical

$\bullet$ —— Experimental

$A_s = A_s' = 0.22$ in^2

$a_b = 0.45$ a

Inelastic Curvature

Ultimate Curvature
$\phi_u \times 10^{-6}$ (in^{-1})

Fig. 3. Comparison of Calculated and Measured Ultimate Curvature versus Ultimate Axial Load.

Fig. 1. General Arrangement.

$2.5 a = 10"$

4"

4"

10"

Fig. 2. Assumed Stress-Strain Diagram of Concrete in Combined Axial Load and Bending.

4 KSI

$\Delta f_c'' = 0.15 f_c''$

$K_2 \mathcal{E}_u$

$C = K_1 \mathcal{E}_u f_c''$

$f_c'' = 0.85 f_c'$

Stress

Strain

$\mathcal{E}_o = 0.002$ $\mathcal{E}_u = 0.0038$

Ultimate Moment
K-in

$P = P_b$ (balancing load)
3 - Specimen S_1-2
4 - Specimen S_2-3

ϕ —— Experimental
$\bullet$ —— Analytical

$A_s = A_s'$ 0.22 in^2 Set S_1
0.33 in^2 Set S_2

$P = 0$ (Pure bending)
1 - Specimen S_1-5
2 - Specimen S_2-5

Inelastic Rotation

Ultimate Rotation
$\theta_u \times 10^{-3}$ rd

Fig. 5. Comparison of Calculated and Measured Ultimate Rotation, Axial Load and Moment.

Sp.No	$M_u/P_u=e_u$ (in.)	Curvature at Yield $\phi_y \times 10^{-4}$ (1/in) Exp.	Anal.	Curvature at Ultimate $\phi_u \times 10^{-4}$ (1/in) Exp.	Anal.	Inelastic Curvature 10^{-4} (1/in) Exp.	Anal.	Rotation at Yield $\theta_y \times 10^{-3}$ (rad) Exp.	Anal.	Rotation at Ultimate $\theta_u \times 10^{-3}$ (rad) Exp.	Anal.	Inelastic Rotation 10^{-3} (rad) Exp.	Anal.	Axial Load Ult. P_u (K) Exp.	Anal.	Moment Ult. M_u (K-in) Exp.	Anal.
Series S1	**p = p' = 0.0137**																
S_1-1	0.40	–	–	6.5	6.0	–	–	–	–	6.5	6.0	–	–	62.0	60.0	24.8	24.0
S_1-2	1.83	17.0	15.3	17.0	16.0	0.0	0.0	16.0	15.3	16.0	15.3	0.0	0.0	31.3	31.0	57.5	57.0
S_1-3	2.50	14.0	13.0	26.0	23.8	12.0	13.8	12.0	13.0	22.0	20.0	10.0	9.74	21.75	21.0	54.4	52.5
S_1-4	5.60	12.0	7.0	48.0	71.5	36.0	64.0	8.0	7.0	36.0	34.6	28.0	27.05	7.3	7.0	39.2	38.8
S_1-5	∞	7.0	6.5	90.0	183.0	83.0	17.64	7.0	6.5	52.0	70.0	43.0	61.0	0.0	0.0	32.5	31.0
Series S2	**p = p' = 0.0206**																
S_2-1	0.4	–	–	3.9	4.0	–	–	–	–	4.1	4.0	–	–	71.0	70.0	28.4	28.0
S_2-2	1.2	–	–	9.2	10.0	–	–	–	–	10.2	10.0	–	–	52.0	50.0	62.4	60.0
S_2-3	2.3	10.5	14.0	16.5	16.0	0.0	0.0	14.2	14.0	14.2	15.3	0.0	0.0	31.5	31.0	72.5	71.5
S_2-4	7.0	7.0	7.6	50.0	68.5	43.0	60.8	9.0	7.60	34.0	33.0	25.0	26.2	7.5	7.3	52.5	51.1
S_2-5	∞	6.0	7.0	70.0	148.0	64.0	141.0	7.0	7.0	43.0	60.0	36.0	50.5	0.0	0.0	46.0	44.0

SUMMARY

The results of this investigation can be summarized as follows:

1. Suitable equations have been developed to accurately predict axial force – bending moment – curvature characteristics. Good agreement was obtained between the calculated strength and deformation values and the corresponding experimental data.

2. Maximum compressive strains of the order of 0.006 existed at extreme fibres near ultimate load, suggesting that larger deformations can be substained at the so-called "flexural hinges". This would lead to a higher degree of moment redistribution in statically indeterminate reinforced concrete systems, which constitutes the basis of limit design.

3. Rotation capacity of the "flexural hinge" was not significantly influenced by the longitudinal steel percentage and was a maximum for the case of pure flexure.

4. Analytical and experimental results show that the available rotation capacity decreased by approximately 25 per cent as the axial compressive load was increased from zero to a point where balanced column failure resulted. Beyond the balance point, available hinge rotation diminished gradually becoming zero for the case of pure axial compression.

RESUME

Les résultats de cette étude peuvent se résumer de la façon suivante:

1. On a développé des équations permettant de prévoir avec précision les interactions force axiale – moment de flexion – courbure. On a obtenu une bonne concordance entre les charges ultimes et les déformations calculées et les résultats expérimentaux.

2. On a constaté, à l'approche de la charge ultime, des déformations de compression maximales de l'ordre de 0.006 dans les fibres extérieures, ce qui conduit à penser qu'on peut obtenir de plus grandes déformations aux rotules plastiques. Cela conduirait à un plus haut degré de redistribution des moments pour les systèmes hyperstatiques en béton armé, ce qui constitue la base du dimensionnement à la limite.

3. La capacité de rotation des rotules plastiques n'a pas été
    influencée de façon décisive par la quantité d'armature
    longitudinale, et s'est avérée maximale dans le cas de la
    flexion pure.

4. Les résultats analytiques et expérimentaux montrent que la
    capacité de rotation diminue d'environ 25% quand on fait
    varier la compression axiale de zéro jusqu'au point d'écou-
    lement simultané des armatures tendues et comprimées. Au
    delà de ce point, la capacité de rotation diminue graduelle-
    ment jusqu'à atteindre zéro pour le cas de la compression
    pure.

ZUSAMMENFASSUNG

    Die Ergebnisse der vorliegenden Untersuchung lassen sich wie
folgt zusammenfassen:

1. Einfache Ausdrücke gestatten die genaue Voraussage der Be-
    ziehungen zwischen Normalkraft, Biegemoment und Krümmung.
    Eine gute Uebereinstimmung zwischen Rechnung und Versuch
    besteht.

2. Randbruchstauchungen der Grössenordnung 0.006 waren in der
    Nähe der Bruchlast zu beobachten und lassen den Schluss zu,
    dass grössere Verformungen im Bereich der sog. plastischen
    Gelenke ertragen werden können. Diese Tatsache lässt eine
    stärkere Momentenumlagerung in statisch unbestimmten Stahl-
    betontragwerken erwarten (Traglastverfahren).

3. Die Rotationsfähigkeit plastischer Gelenke war nicht spürbar
    beeinflusst durch den Längsbewehrungsgehalt und zeigte ein
    Maximum bei reiner Biegung.

4. Rechnerische und Versuchstechnische Ergebnisse zeigen, dass
    die verfügbare Rotationsfähigkeit nur etwa 25% zurückgeht,
    wenn die Normalkraft von Null bis zu derjenigen Last an-
    wächst, bei welcher gleichzeitig sowohl die Druck- als
    auch die Zugbewehrung fliesst. Oberhalb dieser Last ging
    die Rotationsfähigkeit stetig zurück bis auf Null für
    zentrischen Druck.

Leere Seite

Blank page

Page vide